Lukasova *et al. Metab Target Organ Damage* 2024;4:36
DOI: 10.20517/mtod.2024.46

Metabolism and Target Organ Damage

Original Article

Open Access

Check for updates

Onion-skin type of periductular sclerosis in mice with genetic deletion of biliary kindlin-2 as tight junction stabilizer: a pilot experiment indicating a primary sclerosing cholangitis (PSC) phenotype

Martina Lukasova[1], Katharina Weinberger[2], Ralf Weiskirchen[3], Wolfgang Stremmel[4]

[1]Pharmacy of University Clinics of Heidelberg, Ruprecht Karls University Heidelberg, Heidelberg D-69047, Germany.
[2]Institute of Pharmacy and Molecular Biotechnology (IPMB), Ruprecht Karls University Heidelberg, Heidelberg D-69047, Germany.
[3]Institute of Molecular Pathobiochemistry, Experimental Gene Therapy and Clinical Chemistry (IFMPEGKC), RWTH University Hospital Aachen, Aachen D-520741, Germany.
[4]Medical Center Baden-Baden, Baden-Baden D-76530, Germany.

Correspondence to: Dr. Wolfgang Stremmel, Medical Center Baden-Baden, Beethovenstraße 2, Baden-Baden D-76530, Germany. E-mail: wolfgangstremmel@aol.com (WS)

How to cite this article: Lukasova M, Weinberger K, Weiskirchen R, Stremmel W. Onion-skin type of periductular sclerosis in mice with genetic deletion of biliary kindlin-2 as tight junction stabilizer: a pilot experiment indicating a primary sclerosing cholangitis (PSC) phenotype. *Metab Target Organ Damage* 2024;4:36. https://dx.doi.org/10.20517/mtod.2024.46

Received: 6 Jun 2024 **First Decision:** 20 Aug 2024 **Revised:** 4 Sep 2024 **Accepted:** 26 Sep 2024 **Published:** 10 Oct 2024

Academic Editor: Amedeo Lonardo **Copy Editor:** Yu-Fei Wang **Production Editor:** Yu-Fei Wang

Abstract

Aim: Primary sclerosing cholangitis (PSC) and ulcerative colitis are often associated. In ulcerative colitis, a tight junction defect can be detected, resulting in impaired secretion of hydrophobic phosphatidylcholine to the intestinal mucus. This defect causes a vulnerable mucus shield, allowing the microbiota to attack and leading to mucosal inflammation. A similar pathomechanism may be present in PSC.

Methods: To study biliary deletion of tight junctions, mice carrying a Cre/loxP system sensitive to tamoxifen were used to delete kindlin-2, a tight junction adapter protein. The Cre-preceded promoter was derived from hepatocyte nuclear factor-1β (Hnf1β), which is specific for biliary and pancreatic epithelium operative in embryonic life until adolescence. Cre-negative kindlin-2$^{flox/flox}$ mice treated with tamoxifen served as controls.

Results: After tamoxifen induction, alterations in the biliary epithelium were detectable. As a hallmark feature of PSC, an onion-skin type of fibrosis around the bile ducts was present. However, levels of alkaline phosphatase,

bilirubin, aspartate aminotransferase, alanine aminotransferase, and lactate dehydrogenase in the serum were not yet elevated in these young mice.

Conclusion: Genetic deletion of cholangiocyte kindlin-2 impairs tight junctions, revealing a PSC-like phenotype. This supports the hypothesis that an impaired phosphatidylcholine content of biliary mucus allows luminal bile acids to attack the biliary epithelium, leading to cholangitis.

Keywords: Primary sclerosing cholangitis (PSC), tight junctions, kindlin-2, Fermt2, animal model, phosphatidylcholine

INTRODUCTION

Phosphatidylcholine (PC) is a major component of cell membranes and plays critical roles in various physiological processes, including lipid metabolism, inflammation, and cell signaling[1]. Changes in PC physiology can significantly impact metabolic syndrome and conditions such as metabolic-associated steatotic liver disease (MASLD), potentially leading to liver fibrosis[2]. Insufficient PC levels can impair very low density lipoprotein (VLDL) production, leading to fat accumulation in the liver (steatosis) as an early stage of MASLD that can progress to more severe liver damage[3]. It is the ongoing hepatic inflammation resulting from oxidative and endoplasmic reticulum stress due to lipid accumulation that stimulates fibrogenesis. Understanding these mechanisms might offer insights into potential therapeutic targets for managing both metabolic disorders and associated liver conditions.

Another often neglected physiological function of PC relates to its protective property in mucus, where it generates a hydrophobic barrier against luminal aggressors, such as protection against bile acid attack of biliary epithelium or bacterial invasion of intestinal mucosa[4]. The presence of PC in mucus is mediated by tight junctions (TJs)[4]. Lack of mucus PC, as proposed in this study, may be the key inflammatory trigger for fibrogenesis. A classical fibrotic disease of the liver, with a different pathophysiology from MASLD, is primary sclerosing cholangitis (PSC). The notion that disruption of TJ is a pathogenetic feature initially came from studies with the deletion of TJ proteins and the TJ adapter proteins, such as kindlin-2[5-7].

There are several PSC animal models described, induced by chemicals, infectious agents, biliary obstruction, or biliary cell injury[8]. However, the reported genetically modified mouse models do not closely resemble the human type of PSC[9-15]. The hallmark of PSC is the onion-skin type of periductal fibrosis, which, to our knowledge, is rarely found in the available animal models of PSC[8]. Most commonly reported are cholestasis, biliary stenoses, and hepatic inflammation. Although TJ disruption has been described as a cause or consequence of PSC[9,16], an animal model with biliary TJ disruption and development of a PSC phenotype showing the characteristic feature of periductal fibrosis is not currently available.

Previous studies have shown that mice with a deletion of kindlin-2 in the intestinal mucosa reveal a phenotype of ulcerative colitis[17]. The tamoxifen-induced gene deletion led to the destruction of interepithelial TJ, which prohibited the translocation of lipophilic PC originating from lipoproteins in the circulation across the TJ barrier to the intestinal mucus[17,18].

The proposed mechanism regarding the physiology of PC transport into mucus involves the translocation of PC within a lipoprotein-free fraction of blood through endothelial gaps to mucosal tissue[17,18]. In the interstitial space of the intestinal mucosa, the positively charged head group of PC is attracted to the negatively charged TJ between the apical side of mucosal cells. With time, the PC moves by passive flip-flop or through TJ channels to the apical outer surface plasma membrane driven by the negative charge

environment created by cystic fibrosis transmembrane conductance regulator (CFTR) with secretion of Cl^- and HCO_3^-. PC is then bound to membrane-anchored mucin 3, which is highly negatively charged[18]. From there, it is transferred to secretory mucin 2. This mechanism operates mainly in the distal ileum, but the mucus with PC bound to mucin 2 moves to the colon to be discharged with stool[17,18]. This hydrophobic shield protects against the attack of the microbiota[19,20].

In ulcerative colitis, TJs of the ileal mucosa are leaky, PC cannot be transported to the apical mucus layer, and thus, the mucus PC is reduced by 70%, facilitating invasion of the microbiota and subsequent inflammation[21,22]. The fact that ulcerative colitis is often associated with PSC prompted us to assume that - at least in part of the PSC patients - the same type of pathomechanism may also be present in the biliary epithelium with a defect in cholangiocyte TJ[22].

It is proposed that under physiologic conditions, the biliary epithelium is also covered by a mucus shield containing PC bound to mucins to generate a hydrophobic barrier[19,20,22]. Translocation of systemic PC across TJ to biliary mucus is required. Disturbance of TJ-mediated transport of PC to biliary mucus reduces its hydrophobicity and promotes susceptibility toward attacks of bile acids from the biliary lumen. This could be the key factor for the pathogenesis of PSC.

Theoretical consideration for the choice of tamoxifen-inducible Hnf1β-specific deletion of kindlin-2 as an appropriate tool to generate a PSC mouse model

Kindlin-2 represents an adapter protein for the laterally localized TJ, mediating paracellular PC translocation to the apical mucus layer[17,18]. Deletion of kindlin-2 inhibits this PC transport[17,18]. The challenge was to delete kindlin-2 in the cholangiocyte epithelium. In the model used in our study, the Cre recombinase is expressed under the control of the Hnf1 homeobox B (Hnf1β) transcription factor. This promoter is active throughout embryonic life until adolescence[23]. While expressed in various organs such as the kidney, colon, intestine, and testis[24-26], Hnf1β plays a major role in differentiating hepatoblasts into cholangiocytes and is strongly expressed in the biliary epithelium[27]. Indeed, it is claimed that upon targeted deletion of Hnf1β, bile system morphogenesis defects develop[28]. In the above-mentioned study by Rodrigo *et al.*[27], the authors performed tamoxifen-inducible lineage tracing experiments in Hnf1βCreER/R26R$^{Yfp/LacZ}$ mice and showed that Hnf1β is expressed in cells forming ductular epithelia, specifically bile and pancreatic ducts, while the contribution of Hnf1β positive cells to newly generated hepatocytes is low in most liver injury models. The Hnf1β promoter operates in the biliary epithelium and pancreatic ducts[27,28], allowing for the deletion of kindlin-2 in these epithelial cells after exposure to tamoxifen. This targeted deletion of kindlin-2 is expected to inhibit the apical translocation of PC, leading to a disrupted and, thus, leaky mucus layer. This disruption may cause a cholangitis phenotype due to exposure of cholangiocytes to luminal bile acids, while the pancreatic epithelium is less susceptible to inflammation in the absence of bile acids. Moreover, PSC is more prevalent in males[29]. Therefore, 7-week-old male mice were used in our study. The applied strategy was thought to minimize the potential effects of kindlin-2 deletion in other organs, although this cannot be ruled out. Moreover, only mice of young age were chosen because the promoter Hnf1β only operates in embryonic and young adolescent life.

METHODS

Mouse housing and husbandry

Animal studies were conducted following the "ARRIVE" guidelines and were approved by the Heidelberg ethics committee (Regierungspräsidium Karlsruhe, permit number: 35-9185.81/G-152/19). The studies took place at the Interfaculty Biomedicine Research Facility (IBF) at Heidelberg University. Experimental and control mice were housed under identical conditions under germ-free animal housing conditions. They received Rod18 complete diet (Lasvendi, Soest, Germany) *ad libitum* and were kept in conventional caging

with ABBEDD LT-E-001 bedding at 22 ℃ with a 12/12-h light/dark cycle.

Generation and treatment of a tamoxifen-inducible Hnf1β-driven kindlin-2 null mouse model

The Cre-driver mouse strain [Tg(Hnf1b-Cre/ERT2): #027681, Jackson Laboratory] carries a creERT2 fusion gene, replacing exon 1 of the Hnf1β gene. This fusion consists of a Cre recombinase bound to a human estrogen receptor ligand binding domain sensitive to tamoxifen exposure[30]. The mice were backcrossed to a C57BL/6N mice strain at Heidelberg University. The second strain used in our study, kindlin-2$^{flox/flox}$, has *loxP* sites flanking exon 15 of the *Fermt2*/*Kind2* gene, which includes the stop codon and polyadenylation signal[31]. These mice were generously provided by Reinhard Fässler (Max-Planck Institute for Biochemistry, Martinsried, Germany) and were bred on a C57BL/6N background. To minimize the influence of genetic polymorphisms resulting from breeding at different locations or subtle genetic variations[32], we only used and compared results from littermates in our study. Tamoxifen treatment of Cre-positive homozygous kindlin-2$^{flox/flox}$ knockout mice was done at 7 weeks of age because it is close to the time when the Hnf1β promoter is no longer active. They were sacrificed 4 or 8 weeks later, as recommended for this induction procedure[33]. The tamoxifen stock solution (10 mg/mL) was prepared by mixing 40 mg of tamoxifen with 400 μL of ethanol and 3.6 mL of sunflower oil. Each test animal received daily intraperitoneal injections of 2 mg of tamoxifen (200 μL of 10 mg/mL solution) for 5 days. Cre-negative kindlin-2$^{flox/flox}$ mice with tamoxifen treatment were used as controls to eliminate any nonspecific effects of tamoxifen or diluent (10% ethanol/ 90% sunflower oil).

Genotyping of mice

Tissue samples from the ears of F2 generation mice were digested with 3% protein kinase K buffer overnight at 56 ℃ before stopping the reaction at 96 ℃ for 10 min[34]. The concentration of genomic DNA was measured[35,36] and fragments were amplified and tested for the presence of the Cre transgene according to the standard genotyping protocol provided by The Jackson Laboratory for stock #027681[37]. In brief, primers Hnf1b-fw (24230): 5'-CCC ACT TTC TCG GTT TTT CC-3' and Cre-rev (oIMR9074): 5'-AGG CAA ATT TTG GTG TAC GG-3' were used for detection of the Cre recombinase. In this PCR, the presence of Cre recombinase (in a hemizygous or homozygous constellation) results in a ~215 bp amplicon. As internal PCR control, the primers Crtl-fw (21238): 5'-CTG TCC CTG TAT GCC TCT GG-3' and Crtl-rev (21239): 5'-AGA TGG AGA AAG GAC TAG GCT ACA-3' were added in the same PCR reaction, resulting in a 415 bp fragment that originated from an amplification of a fragment located on chromosome 5.To discriminate between wild-type kindlin-2 and floxed kindlin-2 sequences, primers kind2-fw: 5'-AGG GGA TTA ACT GGG TAC CAG-3' and kind2-rev: 5'-GCT GTC ACT GAC TGA CAG TAA CC-3' were used in genotyping PCR. This resulted in the amplification of a 169 bp fragment for the wild-type kindlin-2 allele and a slightly larger product for the kindlin-2 allele that, in addition to the 169 bp, contained two *loxP* sequences. To estimate the size of amplicons, we used the Quick-Load® Purple 1 kb Plus DNA ladder (New England Biolabs GmbH, Frankfurt am Main, Germany) that contains size markers with sizes ranging from 100 bp to 10,002 bp.

Mice analyses

Mice were weighed and then euthanized using carbon dioxide. After sacrificing the animals, blood was collected via heart puncture from the ventricular cavity that typically yielded a fraction of around 0.1 to 0.3 mL of blood. Following the guidelines for analyzing animal models of PSC in blood, serum levels of aspartate aminotransferase (AST), alanine aminotransferase (ALT), lactate dehydrogenase (LDH), bilirubin, and alkaline phosphatase (AP) were measured using standard clinical chemistry tests[8]. Mean values and standard deviations (SD) were reported. A significance level of $P < 0.05$ was considered statistically significant.

The livers were perfused with 10 mL of phosphate buffered saline (PBS), pH 7.4, followed by 20 mL of 4% paraformaldehyde in PBS at pH 7.4. The livers were then removed, weighed, and stored at 4 ℃ until further analysis. For histological examination, the livers were dehydrated, embedded in paraffin, and sectioned into 5 µm slices. The biliary tract was examined in liver sections following the guidelines for animal models of PSC[8]. The largest liver lobe was cut longitudinally in half for hematoxylin and eosin (H&E) staining for conventional histology and Sirius red tissue staining for fibrotic tissue. To quantify periductal fibrosis, the ratio of fibrosis diameter around the corresponding bile duct to the luminal distance of the bile duct was calculated in the same cut direction. Five medium or large bile ducts were selected from liver section printouts for each animal. Six control mice and six kindlin-2-deleted mice were analyzed after 4 or 8 weeks of tamoxifen treatment, with 3 mice in each group. A predetermined cut-off ratio of periductal fibrosis thickness to luminal diameter of 0.5 was considered physiologic, whereas a ratio of periductal fibrosis to luminal diameter of > 0.5 defined a PSC phenotype. The printouts were analyzed blindly by three investigators, and means were calculated for each periductal fibrosis measurement. These means were then compared within each group. Since there was no difference between the 4- and 8-week tamoxifen groups (control and kindlin-2-deleted mice), they were combined for the final analysis (means and SD, $P < 0.05$ was statistically significant).

RESULTS

The topic of PC transport to the biliary mucus has been previously addressed[22]. To introduce the rationale of the present study, it is briefly summarized in Figure 1. In the polarized biliary epithelial cell line Mz-ChA-1 with an intact TJ barrier, it was previously shown that TJs are disrupted by kindlin-2 deletion, leading to diminished apical PC transport [Figure 1][38]. Transmission electron microscopy revealed that the structure of TJ is disturbed. This proof of principle was demonstrated in intestinal mucosa-deleted kindlin-2 mice [Figure 1][17]. In this figure of historic data, we also show the histology of human PSC and the kinetics of PC transport across the TJ barrier to the apical (biliary lumen) side of the polarized human biliary tumor cell line Mz-ChA-1[22,38]. This luminal translocation of choline-containing phospholipids (sphingomyelin is of minor abundance) is driven by the negative charge generated by CFTR and anion exchanger 2 (AE2)[38]. After the transport of PC across the TJ barrier, it is bound to mucins to establish a hydrophobic mucus layer[22,38]. Thus, the generation of a kindlin-2-deleted mouse with specificity to cholangiocytes was expected to reveal a PSC phenotype.

Genotyping and characterization of TJ disruption in kindlin-2-deleted mice

Genotyping was performed using standard PCR with primers for Cre, kindlin-2 (*Fermt2*), and an internal control, followed by gel electrophoresis. This method allowed for the identification of mice with the desired genotypes, including those lacking kindlin-2 (Cre^+/kindlin-$2^{flox/flox}$), as well as control mice (Cre^-/kindlin-$2^{flox/flox}$). The wild-type and floxed kindlin-2 alleles were clearly distinguished through agarose gel electrophoresis, as shown in Figure 2. Phenotypic depletion of TJ proteins using Western blot analysis is a technical challenge because, to our knowledge, pure cholangiocytes have not yet been successfully isolated from mouse liver. Additionally, in total liver, cholangiocytes represent only a small fraction of the total cell population in the liver, which dilutes the signal of cholangiocellular TJ knockout in Western blot analysis. Even immunohistochemistry is difficult to perform with sufficient accuracy.

Biometric description of mice

Each group of six control and kindlin-2-deleted mice was induced at the age of 7 weeks for either 4 weeks (n = 3) or 8 weeks (n = 3) with tamoxifen. All animals appeared to be in good health and were active and mobile in their cages. They did not exhibit any signs of distress, ate and drank normally, and had regular breathing and heart rates. There were no signs of bleeding, and their skin appeared normal. The average body weight of all control mice was 28.0 ± 1.9 g, while that of all kindlin-2-deleted animals was 30.2 ± 5.6 g,

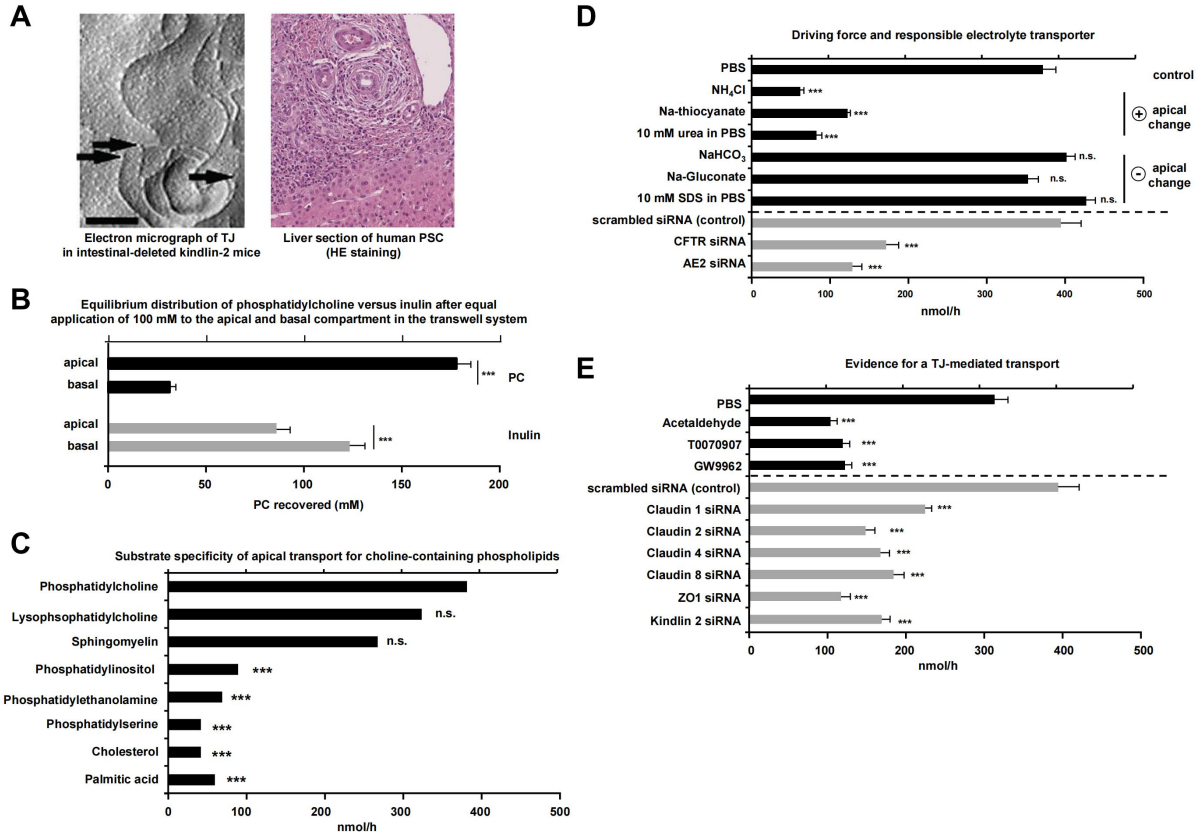

Figure 1. Historical data on the disrupted TJ structure in intestinal kindlin-2-deleted mice, histology of human PSC, and PC transport in the polarized human biliary tumor cell line Mz-ChA-1. (A) On the left, an electron micrograph displays altered TJ architecture in intestinal kindlin-2-deleted mice[17]. On the right, a liver section (HE staining) of human PSC shows the characteristic onion-skin type of periductal fibrosis with cuboidal-shaped cholangiocytes indicating TJ disruption[22]; (B) Substrate transport was assessed using the polarized biliary epithelial tumor cell line Mz-ChA-1 in a transwell tissue culture system[38]. Shown is the equilibrium distribution of PC versus inulin when applied equally at 100 mM to the apical and basal compartments. Over 1-hour incubation, vectorial transport of PC was directed apically, depleting PC at the basal side. In contrast, a significantly higher accumulation of inulin was registered at the basal side; (C) Substrate specificity was examined by assessing apical transport for 1-hour after basal application of different substrates at a 10 mM concentration; (D) The mechanism of apical PC translocation after basal application (10 mM) involved ionic driving forces generated by the apical application of salts and substrates. Anionic and cationic partners permeate the membrane at different velocities, leaving a positive or negative-charged environment at the apical cell surface. The involvement of the responsible anion exporters CFTR and AE2 was proven by their downregulation using respective siRNAs in comparison to scrambled siRNA. PC (10 mM) was applied to the basal compartment; (E) Evidence of TJ involvement in apical transport of PC after their chemical disruption by acetaldehyde vapor or the indicated PPAR-γ inhibitors T0070907 and GW9962. The involvement of the responsible TJ proteins was evaluated by indicated siRNA preincubation in comparison to scrambled siRNA. PC (10 mM) was applied to the basal compartment in polarized Mz-ChA-1 cells. Means ± SD, $n = 6$. Significances were calculated against PBS (control). ***$P < 0.001$. PSC: Primary sclerosing cholangitis; TJ: tight junction; PC: phosphatidylcholine; PBS: phosphate buffered saline; CFTR: cystic fibrosis transmembrane conductance regulator; AE2: anion exchange protein 2; PPAR-γ: peroxisome proliferator-activated receptor-γ.

with no significant difference based on the duration of tamoxifen induction. The same pattern was observed for liver weight, which was 1.8 ± 0.3 g in the untreated group and 1.9 ± 0.3 g in the tamoxifen-treated group.

Serum parameters

The serum of each animal was tested for AST, LDH, ALT, and AP, as well as direct and total bilirubin. However, since direct and total bilirubin levels were almost undetectable, they are not shown here. The results of the different parameters are shown in Table 1.

Table 1. Enzyme values (U/L, means with standard deviation) in serum of control and kindlin-2-deleted mice

	AST	LDH	ALT	AP
Controls (n = 6)	78 ± 34	206 ± 59	36 ± 13	99 ± 15
Kindlin-2-deleted mice (n = 6)	90 ± 51	212 ± 70	30 ± 3	96 ± 17

AST: Aspartate aminotransferase; LDH: lactate dehydrogenase; ALT: alanine aminotransferase; AP: alkaline phosphatase.

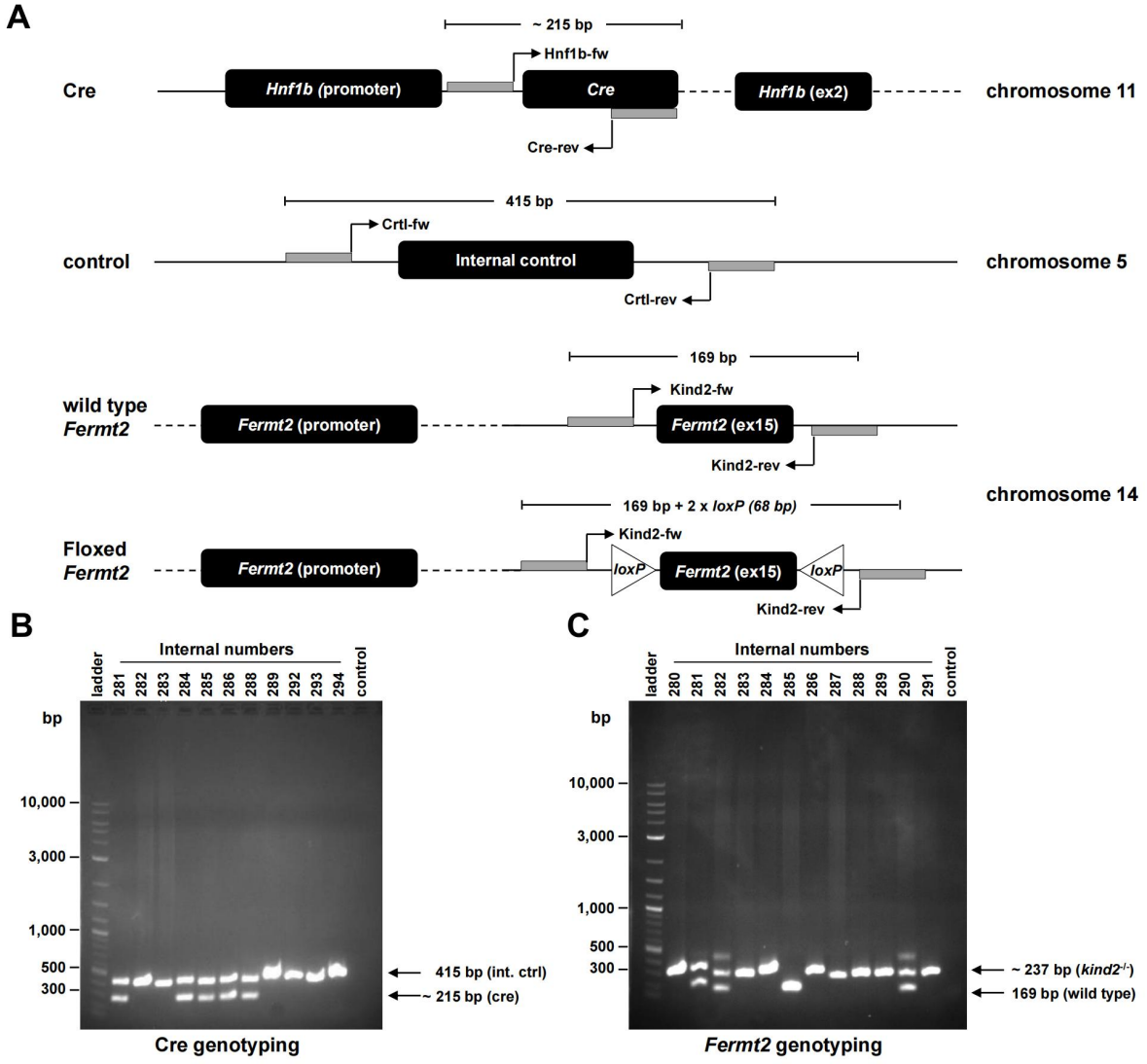

Figure 2. Mouse genotyping strategy used in our study. (A) The locations of primers used for genotyping and the expected sizes of PCR amplicons are shown; (B) DNA isolated from ear punches of mice was genotyped for internal control and Cre transgene. Animals 281, 284, 285, 286, and 288 tested positive, while animals 282, 283, 289, 292, 293, and 294 tested negative for Cre. The 415 bp internal control was amplified in each PCR reaction; (C) DNA isolated from ear punches of mice was genotyped for *kindlin-2 (Fermt2)* wild type and null alleles. Animals 280, 283, 284, 286, 287, 288, 289, and 291 are homozygous for the kindlin-2 null allele, animals 281, 282, and 290 are heterozygous for the null allele, and animal 285 carries two copies of the kindlin-2 wild-type allele. For details on the PCR strategy, please refer to the Material and Methods section. For the images shown in Figure 2B and C, we used 1% agarose gels with a running buffer of 1 x TAE buffer (10 mM Tris, pH 8.0, 0.1 mM EDTA). Gel electrophoresis was performed at 4 °C for 90 min at 140 V. It should be noted that the Cre-preceded promoter that drives deletion of the *kindlin-2 (Fermt 2)* gene was derived from the hepatocyte nuclear *factor-1β* (*Hnf1β*) gene, which is active only in biliary and pancreatic epithelium operative in embryonic life until adolescence. CRTL: Control; KIND2: kindlin-2.

In all cohorts, the tested enzymes were within a comparable range with no difference after 4 and 8 weeks of tamoxifen exposure ($P > 0.05$ between control and kindlin-2-deleted mice, whether they were under tamoxifen for 4 or 8 weeks). The obtained values were in the normal range[39,40]. Standard deviations were narrow for ALT (an indicator of hepatocellular injury) and AP (an indicator of cholestasis), whereas they were higher for AST and LDH, most likely due to different degrees of hemolysis when blood was taken by heart puncture. The observation indicates that 4 and 8 weeks after tamoxifen induction, the kindlin-2-deleted mice did not show any signs of clinically obvious cholestasis or inflammation. Cholestatic and liver enzymes are expected to rise later in the course of the disease.

The macroscopic appearance of explanted livers of kindlin-2-deleted mice

The livers of the kindlin-2-deleted mice compared to controls showed a marbled pale structure [Figure 3], possibly indicating an increase in periductal fibrosis. In contrast, all other organs of kindlin-2-deleted mice, including the pancreas, appeared macroscopically normal with no visible abnormalities.

Histology of control and kindlin-2-deleted mice

Control and kindlin-2-deleted mice were evaluated after induction with tamoxifen for either 4 or 8 weeks. There was no difference between the 4- and 8-week induction periods. Representative data from two sets of experiments (7-week-old mice induced by tamoxifen for 8 weeks) are shown in Figures 4-6. The appearance of PSC showing various degrees of onion-skin fibrosis around the bile ducts differed, even within the same liver [Figure 6]. At higher magnification, the biliary epithelial cells of human PSC [Figure 1] and kindlin-2-deleted mice revealed a more cuboidal shape compared to controls, an indirect sign of TJ disturbance due to impairment of lateral cell contacts[17].

Sirius red staining revealed a significant increase in collagen deposition after depletion of kindlin-2, as indicated by the red staining, while the background appeared yellow. This observation confirms the presence of increased collagen in the onion-skin fibrosis pattern. The semiquantitative determination of the ratio of the thickness of periductal fibrosis to the luminal diameter of the corresponding bile duct (measured in the same cut direction) further supported this finding. In kindlin-2-deleted mice, the values were > 0.5 (2.4 ± 1.8), compared to controls with values < 0.5 (0.15 ± 0.07) ($P < 0.005$) ($n = 30$ in each group).

DISCUSSION

The genetic mouse model and its PSC-like phenotype

The present study demonstrates that the strategy of cholangiocellular deletion of kindin-2 as a TJ adapter protein could cause TJ disruption in the chosen genetic mouse model. Indeed, it resulted in an onion-skin type of fibrosis around the bile ducts, similar to that found in human PSC[41-43].

The logic of previous experiments led us to delete TJ in cholangiocyte epithelium in a genetic mouse model with kindlin-2 deletion to impair mucus PC secretion, even though we were unable to demonstrate structural disruption of TJs for technical reasons because of low abundancy and difficulty in identifying cholangiocytes. However, in intestinally deleted kindlin-2 mice, disorganization of TJ was shown, which we considered a proof-of-principle [Figure 1][17]. One additional indication could be the observation that the shape of biliary epithelial cells in kindlin-2-deleted mice and in human PSC [Figure 1] appeared more cuboidal at higher magnifications compared to controls, similar to intestinal mucosa deletion of kindlin-2[17]. It suggests that the close lateral attachment of the cells is loosened, which allows the cholangiocytes to expand to a more rounded shape. However, it is only an indirect criterion. Disturbed TJs weaken the barrier function against the attack of luminal bile acids[38].

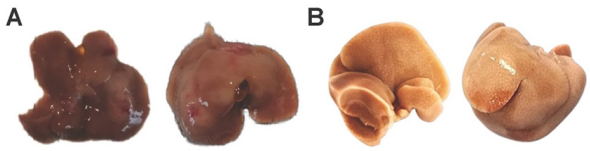

Figure 3. Phenotypic appearance of a kindlin-2-deleted liver. The images show the livers of a normal (A) and a kindlin-2-deleted (B) mouse from two different views.

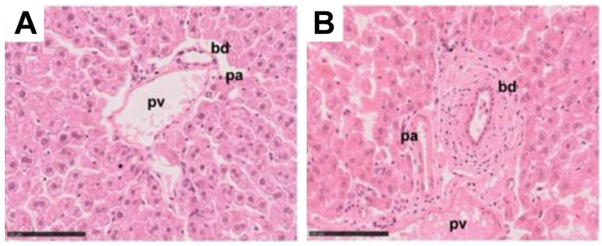

Figure 4. Hematoxylin and eosin staining of liver sections of 8-week tamoxifen-induced control (A) and kindlin-2-deleted (B) mice. The controls displayed normal bile ducts, whereas the knockout mice exhibited the characteristic onion-skin type of fibrosis around the bile ducts. Space bare are 100 μm. BD: Bile duct; PA: portal artery; PV: portal vein.

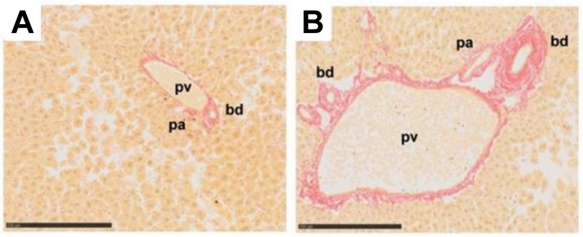

Figure 5. Sirius red staining of liver sections from 8-week tamoxifen-induced control (A) and kindlin-2-deleted (B) mice. The control mice displayed normal bile ducts, while the kindlin-2-deleted mice exhibited a characteristic onion-skin type of fibrosis around the bile ducts. Space bars are 250 μm. BD: Bile duct; PA: portal artery; PV: portal vein.

The question of how the barrier function is established is quite intriguing. In kinetic studies conducted with the human cholangiocellular carcinoma-derived cell line Mz-ChA-1, a new concept has been developed. It suggests that PC is transported from systemic sources (lipoproteins in blood) to the biliary mucus, where it helps to maintain a barrier function toward the biliary lumen. This transport of PC to the biliary mucus has been demonstrated in a transwell culture system with the polarized biliary tumor cell line Mz-ChA-1, following a similar process as described for the intestinal mucosa[38]. In conjunction with CFTR, the nonerythroid anion exchanger AE2/solute carrier family 4 member 2 (AE2 encoded by the *SLC4A2* gene) transports Cl^- and HCO_3^- apically, creating what is referred to as 'the biliary bicarbonate umbrella'[44,45]. The accumulation of negative charge provides the driving force to move PC across TJ for binding to mucin 3 and secretory mucin 2. When TJs are disrupted, PC translocation to the mucus is hindered, reducing its repelling hydrophobicity. This allows bile acids to attack cholangiocytes, leading to portal inflammation and, subsequently, to periductal fibrosis[22] [Figure 7]. This narrowing of the biliary lumen, along with impaired motility due to tissue stiffness, exacerbates cholestasis and perpetuates inflammation, ultimately leading to cirrhosis with a high risk of cholangiocellular carcinoma development, as has been well established for human PSC[41-43,46].

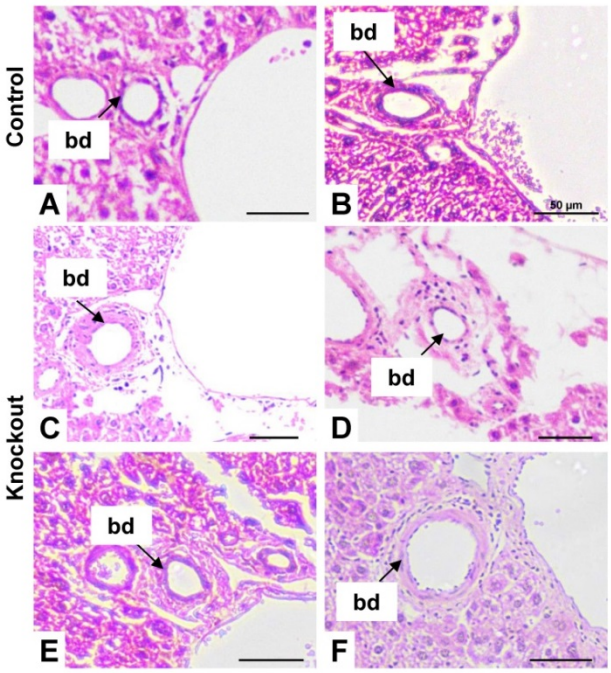

Figure 6. H&E staining of liver sections. Sections from control mice after four (A) and eight weeks (B) after tamoxifen induction are depicted. Here, the single layer of epithelial cells is without surrounding fibrosis. In contrast, the lower panel shows in (C-F) kindlin-2-deleted mice with different degrees of periductular onion-skin type of fibrosis around the epithelial surface layer. Images in (C) and (D) were taken from animals four weeks after tamoxifen induction and in (E) and (F) from animals eight weeks after tamoxifen treatment. The layers of periductal fibrosis, also seen in Figures 4 and 5, vary in the kindlin-2 knockout mice, reflecting a multitude of histologic phenotypes. Comparable to human PSC, histologic lesions are spotty and consistent with different stages of PSC that can be present in a single liver simultaneously. There was no difference between the animals regarding serum markers of cholestasis and inflammation. Original magnification 100 x. Scale bars represent 50 µm. BD: Bile duct. PSC: primary sclerosing cholangitis.

The apical translocation of PC between biliary epithelial cells is comparable to its secretion into intestinal mucus as described in the introduction. It is noteworthy that this transport is disrupted in ulcerative colitis with its high association with PSC. One could argue that both diseases, at least in a subgroup of patients, share a common pathophysiology that could be classified as 'tight junctional disease'[22].

The published mechanism, along with the *in vivo* disruption of TJ by mucosal cell deletion of kindin-2 leading to an ulcerative colitis phenotype, inspired us to conduct this study. We hypothesized that luminal bile acids penetrate the PC-depleted and, thus, leaky mucus layer, hitting the cholangiocyte cell layer from the apical side, leading to their destruction. Repair mechanisms induce subepithelial fibrosis. This localization likely results from the overactivation of portal myofibroblasts rather than hepatic stellate cells, although this was not proven in the present study. Porto-portal septa develop, and regeneration of cholangiocytes is expected, causing ductular proliferation. These kindlin-2-deficient cells, lacking TJ and protective PC secretion, are again attacked by mucus-penetrating bile acids, followed by another round of repair. This perpetuating mechanism eventually results in an onion-skin type of periductal fibrosis, the hallmark of PSC, although it may not be detectable in all cases[41-43,46]. The layers of periductal fibrosis vary among different PSC patients and even within the liver of an individual patient, as also seen in our mouse PSC model, although the increase in fibrotic tissue was always observed [Figures 4-6].

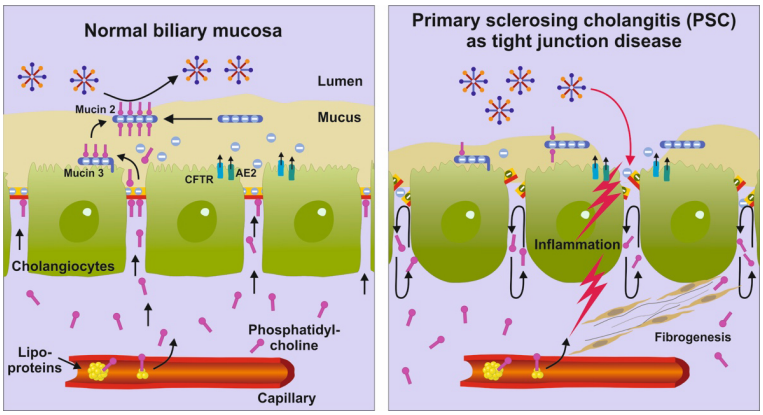

Figure 7. A hypothesis on the pathophysiology of PSC. PC in mucus originates from systemic sources. Within a lipoprotein-free fraction, PC travels out of the capillaries through endothelial gaps and distributes in the interstitial spaces between cholangiocytes, into which PC cannot enter due to its complex structure. With its positively charged head group, PC is drawn to the negatively charged TJ. Over time, PC accumulates and passes through the protein strands of the TJ to the outer surface of cholangiocytes driven by the negative charge generated by CFTR and AE2. PC then binds to mucin 3, which is anchored in the external plasma membrane, before being transferred to secretory mucin 2 to move further distally within the mucus of the biliary channel system. In cases of TJ disease, the attraction to TJ proteins fails, preventing the outward movement of PC. Any disruption in the complex PC secretion mechanism, particularly the binding to the TJ, can lead to insufficient PC accumulation in biliary mucus. This lack of mucus hydrophobicity results in a defective mucus barrier, allowing bile acids from the biliary lumen to harm cholangiocytes. This leads to an inflammatory response (cholangitis) and activates repair mechanisms like fibrosis, as is typical of PSC. Ultimately, this allows for bacterial invasion and the progression of the disease[43,46]. This image was modified from[38]. PC: Phosphatidylcholine; PSC: primary sclerosing cholangitis; TJ: tight junction; CFTR: cystic fibrosis transmembrane conductance regulator; AE2: anion exchange protein 2.

It is remarkable that despite observing typical histologic alterations in the biliary system, the cholestatic enzyme alkaline phosphatase (AP) and bilirubin levels (which were undetectable) remained normal in the present study. It is important to note that the first consequence of the genetic defect chosen leads to a disrupted molecular mechanism of PC secretion, resulting in histologic alterations limited to the biliary epithelium and local fibrotic repair. Only when a critical level of biliary obstruction is reached does cholestasis develop. This suggests that elevated AP already indicates a progressive state of cholestasis. For PSC, the primary event is the typical onion-skin type of fibrosis, with cholestasis being the subsequent step. It is surprising that no alterations in any biomarkers of liver injury were detectable, particularly transaminases (AST, ALT) and LDH, which remained within the normal range. This indicates that hepatic parenchymal inflammation is not yet present and would be the next step after cholestasis. Even in humans, transaminases are only slightly elevated and often late during the course of PSC. However, it is expected that further extending the kindlin-2 deletion will reveal inflammatory and cholestatic responses, when a promoter that operates throughout the lifespan of the mice can be utilized.

At this point, it should be stressed that the molecular pathogenesis of PSC is far from being understood. The present pilot study is simply a hypothetical suggestion based on previous experiments. Further studies are necessary to prove the concept.

Further limitations of the present study

It should be critically noted that we used inbred mice with potentially different genetic backgrounds. The kindlin-2$^{flox/flox}$ mice were bred on a C57BL/6N genetic background, while the Cre driver mouse was created by the microinjection of a transgene into the pronuclei of C57BL6/SJL eggs[30]. Despite multiple backcrosses to C57BL/6N, an exact genetic background match between the two mouse strains used in our study is not guaranteed. It may have an impact on the observed phenotypes because genetic variation and environmental factors can modulate susceptibility to hepatic disease[47,48]. However, by using littermates of

both mouse strains in our experiment, we minimized the risk of phenotypic variations. While it is possible that slight modifications in the genetic background may have affected the mice's phenotype in our study, the detailed description of the mice used should be adequate for study replication. The sample size and analytical procedures are insufficient for definitive conclusions. Many aspects of PSC remain unexplored. The most desirable would be the confirmation of a low biliary mucus PC concentration, as it is the key pathogenetic feature in PSC and in this proposed mouse model. Technically, this is beyond our experimental capabilities and should be performed in specialized laboratories. In particular, the time course of kindlin-2 depletion in cholangiocytes should be better investigated by immunohistochemistry in our model system. It would also be interesting to define the molecular changes that occur in primary cholangiocytes lacking kindlin-2. Other shortcomings relate to the understanding of disease progression and time course-dependent elevation of laboratory parameters (AST, ALT, AP, and LDH), mechanism of cholestasis, reasons for onion-type fibrosis, cirrhosis and cholangiocellular carcinoma development, and the impact of therapy on disease progression.

Future experimental and functional aspects of the model used in this study

Experimental

Specialized laboratories with more advanced technologies are now needed to reproduce our results and analyze the animals as proposed for PSC genetic mouse models throughout the course of the disease[8]. A promising approach could involve monitoring mice after tamoxifen induction by magnetic resonance imaging using gadoxetate[49]. This technique can be performed on living animals, allowing the imaging of large bile ducts over time. It may also provide information about the long-term effects of a TJ knockout. Of particular importance is the documentation of PSC as a TJ disorder at both the structural and functional levels. The demonstration of a defective apical PC translocation across the defective TJ barrier into the mucus is desirable.

Functional implication for therapy

The orally provided PC is not able to pass to the PC deficient biliary mucus as disturbed PC transport due to the postulated TJ defect is the proposed key pathogenetic player in PSC. One strategy could be the application of bile acids, which undergo cholehepatic shunting[50]. In brief, bile acids are physiologically translocated from the liver parenchymal cells across the hepatocellular canalicular plasma membrane via the bile salt export pump (i.e., BSEP, *ABCB11*) into the bile and subsequently bound to biliary PC, which is excreted from hepatocytes via MDR3 (ABCB4). Both constitute bile salt PC micelles. Most of these micelles pass through the biliary tree to the duodenum to mediate fatty acid absorption. Biliary excreted bile acids, which are not conjugated in hepatocytes because of poor affinity for coenzyme A synthetase, are readily taken up by the biliary epithelium due to the high lipophilicity of the protonated acid. After passage through cholangiocytes, they are recirculated via the periductular plexus to the liver. The perpetuation of hepatocellular secretion into bile and reabsorption through biliary epithelial cells leads to their hepatic/biliary circulation (cholehepatic shunt), which enhances bile flow [Figure 8]. Regarding the accompanying PC secretion, it would mean that it is left behind in the biliary lumen after unconjugated bile acids have been absorbed[22]. As a complex lipid, it cannot be taken up by cholangiocytes and would be available to fill up empty PC binding sites on mucin 2 from the biliary luminal side[22,38]. Thus, a hydrophobic mucus shield can be reestablished. Eventually, this could reverse the damage to the biliary epithelium. Indeed, the application of norUDCA, as an example of a bile acid with enhanced cholehepatic shunting, showed promising therapeutic benefits in initial trials in patients with PSC, although the mucus protective mode of action has not been addressed yet[51].

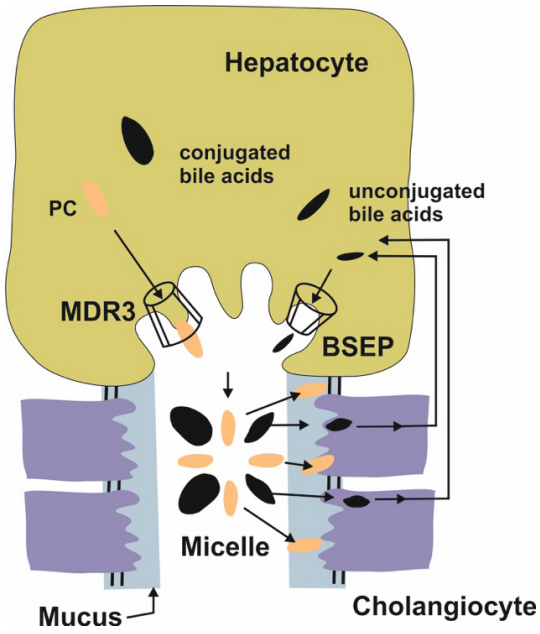

Figure 8. The cholehepatic shunt. Illustrated is the hepatic secretion process of PC through the ABC transporter MDR3 (ABCB4) of the canalicular plasma membrane into the biliary lumen. Additionally, conjugated (fat symbols) and unconjugated (lean symbols) bile acids are secreted through the ABC transporter BSEP (ABCB11) into bile. These substances combine to form micelles that travel down the biliary system to the intestinal lumen for fat absorption. Unconjugated bile acids, which are more lipophilic, are reabsorbed by cholangiocytes and recirculated back to hepatocytes via the periductular plexus. Once taken up by hepatocytes, they are excreted again in bile, enhancing bile flow through this mechanism (cholehepatic shunt). The accompanying phosphatidylcholine remains in the biliary lumen and is available to occupy empty binding sites for phosphatidylcholine on mucin 2, compensating for its absence in mucus and reestablishing a protective hydrophobic barrier. PC: Phosphatidylcholine.

Conclusion

Liver fibrogenesis is always the result of ongoing inflammation. Hepatocellular inflammation causes fibrosis in MASLD. In this case, the intracellular lack of PC causes metabolic and inflammatory response mechanisms that ultimately lead to fibrosis. Fibrosis is also the hallmark of PSC, characterized by a biliary type of inflammation, for which the underlying defect has remained unknown until now. It represents another pathogenetic mechanism of fibrosis originating from the extracellular biliary lumen side of the biliary epithelium caused by a lack of mucus PC. The development of an onion-skin type of periductal fibrosis in the liver of cholangiocellular kindlin-2-deleted mice is the most appropriate description of the finding in the study presented here. Kindlin-2 is a stabilizing component of the TJ barrier between cholangiocytes, which as a whole serves as the exit gate of systemic PC to the biliary mucus. Thus, any disturbance of TJ could cause a PC-deficient biliary mucus layer, allowing bile acids to attack cholangiocytes from the biliary lumen. Despite the lack of evidence of deficient mucus PC content due to experimental obstacles, it is a likely hypothesis derived from intestinal mucosa experiments. Subsequent inflammation of the biliary epithelium triggers fibrogenesis. Therefore, the unique hallmark feature of PSC is the detection of onion-skin type of periductal fibrosis, as shown here, which is suggestive of a pathogenetic link to human PSC. The adolescent age of the mice could explain the lack of biochemical signs of cholestasis and liver injury. There are still many questions that need to be answered by further experiments. However, the road is prepared by a mouse model where an onion-skin type of fibrosis is detectable.

DECLARATIONS

Acknowledgments

The authors are grateful to Professor Reinhard Fässler (Max-Planck Institute for Biochemistry, Martinsried,

Germany), who kindly provided kindlin-2$^{flox/flox}$ mice for the study.

Authors' contributions

Conceptualization: Stremmel W
Validation: Lukasova M, Weinberger K, and Stremmel W
Formal analysis: Lukasova M, Weinberger K, Weiskirchen R, and Stremmel W
Investigation: Lukasova M and Weinberger K
Resources: Stremmel W
Data curation: Lukasova M and Weinberger K
Writing - original draft preparation: Stremmel W and Weiskirchen R
Writing - review and editing: Lukasova M, Weinberger K, Weiskirchen R, and Stremmel W
Visualization: Lukasova M, Weinberger K, and Weiskirchen R
Supervision: Stremmel W
Project administration: Stremmel W
All authors have read and agreed to the published version of the manuscript.

Availability of data and materials

Original data for this study are available from the corresponding author upon reasonable request.

Financial support and sponsorship

Not applicable.

Conflicts of interest

The authors declared there are no conflicts of interest.

Ethical approval and consent to participate

Animal studies were conducted following the "ARRIVE" guidelines and were approved by the Heidelberg ethics committee (Regierungspräsidium Karlsruhe, permit number: 35-9185.81/G-152/19).

Consent for publication

Not applicable.

REFERENCES

1. der Veen JN, Kennelly JP, Wan S, Vance JE, Vance DE, Jacobs RL. The critical role of phosphatidylcholine and phosphatidylethanolamine metabolism in health and disease. *Biochim Biophys Acta Biomembr* 2017;1859:1558-72. DOI PubMed
2. Sánchez V, Baumann A, Brandt A, Wodak MF, Staltner R, Bergheim I. Oral supplementation of phosphatidylcholine attenuates the onset of a diet-induced metabolic dysfunction-associated steatohepatitis in female C57BL/6J mice. *Cell Mol Gastroenterol Hepatol* 2024;17:785-800. DOI PubMed PMC
3. Osipova D, Kokoreva K, Lazebnik L, et al. Regression of liver steatosis following phosphatidylcholine administration: a review of molecular and metabolic pathways involved. *Front Pharmacol* 2022;13:797923. DOI PubMed PMC
4. Stremmel W, Ehehalt R, Staffer S, et al. Mucosal protection by phosphatidylcholine. *Dig Dis* 2012;30 Suppl 3:85-91. DOI
5. Miele L, Valenza V, La Torre G, et al. Increased intestinal permeability and tight junction alterations in nonalcoholic fatty liver disease. *Hepatology* 2009;49:1877-87. DOI
6. Xin D, Zong-Shun L, Bang-Mao W, Lu Z. Expression of intestinal tight junction proteins in patients with non-alcoholic fatty liver disease. *Hepatogastroenterology* 2014;61:136-40. PubMed
7. Zhong Y, Zhou L, Wang H, et al. Kindlin-2 maintains liver homeostasis by regulating GSTP1-OPN-mediated oxidative stress and inflammation in mice. *J Biol Chem* 2024;300:105601. DOI PubMed PMC
8. Fickert P, Pollheimer MJ, Beuers U, et al; International PSC Study Group (IPSCSG). Characterization of animal models for primary

sclerosing cholangitis (PSC). *J Hepatol* 2014;60:1290-303. DOI PubMed PMC
9. Fickert P, Fuchsbichler A, Wagner M, et al. Regurgitation of bile acids from leaky bile ducts causes sclerosing cholangitis in Mdr2 (Abcb4) knockout mice. *Gastroenterology* 2004;127:261-74. DOI
10. Smit JJ, Schinkel AH, Oude Elferink RP, et al. Homozygous disruption of the murine mdr2 P-glycoprotein gene leads to a complete absence of phospholipid from bile and to liver disease. *Cell* 1993;75:451-62. DOI PubMed PMC
11. Durie PR, Kent G, Phillips MJ, Ackerley CA. Characteristic multiorgan pathology of cystic fibrosis in a long-living cystic fibrosis transmembrane regulator knockout murine model. *Am J Pathol* 2004;164:1481-93. DOI PubMed PMC
12. Blanco PG, Zaman MM, Junaidi O, et al. Induction of colitis in cftr-/- mice results in bile duct injury. *Am J Physiol Gastrointest Liver Physiol* 2004;287:G491-6. DOI PubMed
13. Meerman L, Koopen NR, Bloks V, et al. Biliary fibrosis associated with altered bile composition in a mouse model of erythropoietic protoporphyria. *Gastroenterology* 1999;117:696-705. DOI
14. Libbrecht L, Meerman L, Kuipers F, Roskams T, Desmet V, Jansen P. Liver pathology and hepatocarcinogenesis in a long-term mouse model of erythropoietic protoporphyria. *J Pathol* 2003;199:191-200. DOI PubMed
15. Hatano R, Takeda A, Abe Y, et al. Loss of ezrin expression reduced the susceptibility to the glomerular injury in mice. *Sci Rep* 2018;8:4512. DOI PubMed PMC
16. Sakisaka S, Kawaguchi T, Taniguchi E, et al. Alterations in tight junctions differ between primary biliary cirrhosis and primary sclerosing cholangitis. *Hepatology* 2001;33:1460-8. DOI
17. Stremmel W, Staffer S, Schneider MJ, et al. Genetic mouse models with intestinal-specific tight junction deletion resemble an ulcerative colitis phenotype. *J Crohns Colitis* 2017;11:1247-57. DOI PubMed PMC
18. Stremmel W, Staffer S, Gan-Schreier H, Wannhoff A, Bach M, Gauss A. Phosphatidylcholine passes through lateral tight junctions for paracellular transport to the apical side of the polarized intestinal tumor cell-line CaCo2. *Biochim Biophys Acta* 2016;1861:1161-9. DOI
19. Johansson ME, Sjövall H, Hansson GC. The gastrointestinal mucus system in health and disease. *Nat Rev Gastroenterol Hepatol* 2013;10:352-61. DOI PubMed PMC
20. Lichtenberger LM. The hydrophobic barrier properties of gastrointestinal mucus. *Annu Rev Physiol* 1995;57:565-83. DOI PubMed
21. Ehehalt R, Wagenblast J, Erben G, et al. Phosphatidylcholine and lysophosphatidylcholine in intestinal mucus of ulcerative colitis patients. A quantitative approach by nanoElectrospray-tandem mass spectrometry. *Scand J Gastroenterol* 2004;39:737-42. DOI
22. Stremmel W, Lukasova M, Weiskirchen R. The neglected biliary mucus and its phosphatidylcholine content: a putative player in pathogenesis of primary cholangitis-a narrative review article. *Ann Transl Med* 2021;9:738. DOI PubMed PMC
23. El-Khairi R, Vallier L. The role of hepatocyte nuclear factor 1β in disease and development. *Diabetes Obes Metab* 2016;18 Suppl 1:23-32. DOI PubMed
24. Ferrè S, Igarashi P. New insights into the role of Hnf-1β in kidney (patho)physiology. *Pediatr Nephrol* 2019;34:1325-35. DOI PubMed PMC
25. Mouse ENCODE transcriptome data. Available from: https://www.ncbi.nlm.nih.gov/gene?Db=gene&Cmd=DetailsSearch&Term=21410. [Last accessed on 8 Oct 2024].
26. Tholen LE, Latta F, Martens JHA, Hoenderop JGJ, de Baaij JHF. Transcription factor Hnf1β controls a transcriptional network regulating kidney cell structure and tight junction integrity. *Am J Physiol Renal Physiol* 2023;324:F211-24. DOI PubMed
27. Rodrigo-Torres D, Affò S, Coll M, et al. The biliary epithelium gives rise to liver progenitor cells. *Hepatology* 2014;60:1367-77. DOI PubMed PMC
28. Coffinier C, Gresh L, Fiette L, et al. Bile system morphogenesis defects and liver dysfunction upon targeted deletion of Hnf1beta. *Development* 2002;129:1829-38. DOI
29. Invernizzi F, Cilla M, Trapani S, et al; Special Interest Group Gender in Hepatology of the Italian Association for the Study of the Liver (AISF). Gender and autoimmune liver diseases: relevant aspects in clinical practice. *J Pers Med* 2022;12:925. DOI PubMed PMC
30. Solar M, Cardalda C, Houbracken I, et al. Pancreatic exocrine duct cells give rise to insulin-producing beta cells during embryogenesis but not after birth. *Dev Cell* 2009;17:849-60. DOI PubMed
31. Theodosiou M, Widmaier M, Böttcher RT, et al. Kindlin-2 cooperates with talin to activate integrins and induces cell spreading by directly binding paxillin. *Elife* 2016;5:e10130. DOI PubMed PMC
32. Hillebrandt S, Wasmuth HE, Weiskirchen R, et al. Complement factor 5 is a quantitative trait gene that modifies liver fibrogenesis in mice and humans. *Nat Genet* 2005;37:835-43. DOI
33. Ray MK, Fagan SP, Brunicardi FC. The Cre-loxP system: a versatile tool for targeting genes in a cell- and stage-specific manner. *Cell Transplant* 2000;9:805-15. DOI PubMed
34. Ren S, Li M, Cai H, Hudgins S, Furth PA. A simplified method to prepare PCR template DNA for screening of transgenic and knockout mice. *Contemp Top Lab Anim Sci* 2001;40:27-30. DOI PubMed
35. Gopalkrishna V, Francis A, Sharma JK, Das BC. A simple and rapid method of high quantity DNA isolation from cervical scrapes for detection of human papillomavirus infection. *J Virol Methods* 1992;36:63-72. DOI PubMed
36. Boesenberg-smith KA, Pessarakli MM, Wolk DM. Assessment of DNA yield and purity: an overlooked detail of PCR troubleshooting. *Clinical Microbiology Newsletter* 2012;34:1-6. DOI
37. The Jackson Laboratory. Stock Tg(Hnf1b-cre/ERT2)1Jfer/J. Available from: https://www.jax.org/strain/027681 [Last accessed on 8

Oct 2024].

38. Stremmel W, Staffer S, Weiskirchen R. Phosphatidylcholine passes by paracellular transport to the apical side of the polarized biliary tumor cell line Mz-ChA-1. *Int J Mol Sci* 2019;20:4034. DOI PubMed PMC
39. Harrison SD Jr, Burdeshaw JA, Crosby RG, Cusic AM, Denine EP. Hematology and clinical chemistry reference values for C57BL/6 X DBA/2 F1 mice. *Cancer Res* 1978;38:2636-39. DOI PubMed
40. Otto GP, Rathkolb B, Oestereicher MA, Lengger CJ, Moerth C, Micklich K, et al. Clinical chemistry reference intervals for C57BL/6J, C57BL/6N, and C3HeB/FeJ mice (mus musculus). *J Am Assoc Lab Anim Sci* 2016;55:375-86. PubMed PMC
41. Lindor KD, Kowdley KV, Harrison ME; American college of gastroenterology. ACG clinical guideline: primary sclerosing cholangitis. *Am J Gastroenterol* 2015;110:646-59. DOI PubMed
42. Lindström L, Hultcrantz R, Boberg KM, Friis-Liby I, Bergquist A. Association between reduced levels of alkaline phosphatase and survival times of patients with primary sclerosing cholangitis. *Clin Gastroenterol Hepatol* 2013;11:841-6. DOI PubMed
43. Takakura WR, Tabibian JH, Bowlus CL. The evolution of natural history of primary sclerosing cholangitis. *Curr Opin Gastroenterol* 2017;33:71-7. DOI PubMed PMC
44. Banales JM, Prieto J, Medina JF. Cholangiocyte anion exchange and biliary bicarbonate excretion. *World J Gastroenterol* 2006;12:3496-511. DOI PubMed PMC
45. Hohenester S, Wenniger LM, Paulusma CC, et al. A biliary HCO3- umbrella constitutes a protective mechanism against bile acid-induced injury in human cholangiocytes. *Hepatology* 2012;55:173-83. DOI PubMed
46. Karlsen TH, Folseraas T, Thorburn D, Vesterhus M. Primary sclerosing cholangitis - a comprehensive review. *J Hepatol* 2017;67:1298-323. DOI PubMed
47. Benavides F, Rülicke T, Prins JB, et al. Genetic quality assurance and genetic monitoring of laboratory mice and rats: FELASA working group report. *Lab Anim* 2020;54:135-48. DOI PubMed PMC
48. NC3Rs. National Centre for the Replacement Refinement & Reduction of Animals in Research. The importance of background strains in GA mice. Available from: https://nc3rs.org.uk/3rs-resources/importance-background-strains-ga-mice [Last accessed on 8 Oct 2024].
49. Leyendecker JR. Gadoxetate disodium for contrast magnetic resonance imaging of the liver. *Gastroenterol Hepatol* 2009;5:698. DOI PubMed PMC
50. Beuers U, Kullak-Ublick GA, Pusl T, Rauws ER, Rust C. Medical treatment of primary sclerosing cholangitis: a role for novel bile acids and other (post-)transcriptional modulators? *Clin Rev Allergy Immunol* 2009;36:52-61. DOI PubMed
51. Fickert P, Hirschfield GM, Denk G, et al; European PSC norUDCA Study Group. norUrsodeoxycholic acid improves cholestasis in primary sclerosing cholangitis. *J Hepatol* 2017;67:549-58. DOI